

## 3. Liquid-crystal-based tunable terahertz phase shifter/retarder

### 3.1. Introduction

In the past decade, sub-millimeter wave or THz technology has [1] undergone remarkable growth with intense interests for their applications in time-domain far-infrared spectroscopy [2,3], imaging [4], ranging [5] and bio-medical [6] applications. These applications require a variety of active and passive THz optical elements such as polarizers, attenuators, modulators and phase shifters, which are rarely explored up to now. Perforated flat plates that acting as dichroic filters or frequency selective surfaces in the THz range were reported by Winnewisser *et al* [7], however, they were not tunable. For tunable phase shifting application, Libon *et al.* [8] recently demonstrated a device based on optically induced change of the carrier concentration in GaAs multiple quantum well (MQW) structures. Control of the electron occupation and hence absorption of the THz radiation in MQW by an applied electric field has been used by Kersting *et al* [9] to shift the phase of the THz wave. Gated two-dimensional electron gas in semiconductor nanostructures was proposed to change the phase of the THz carrier wave by up to 0.5 radians[10]. These quantum-well-based THz phase shifters, however, operated at temperatures far below room temperature.

The birefringence of liquid crystals (LCs) is well known and extensively utilized in optical systems for control and manipulation of visible, infrared and millimeter wave beams. Indeed, several groups have employed liquid crystals successfully for phase shifting of microwave and millimeter wave signals previously [11,12]. We have recently determined the complex index of refraction of a nematic LC 4'-n-pentyl-4-

cyanobiphenyl (5CB, Merck) [13] or E7 (Daily Corp.) [14] at room temperature by THz time-domain spectroscopy (THz-TDS). Significantly, we show that nematic 5CB and E7 exhibits relatively large birefringence ( $\sim 0.2$ ) and small extinction coefficient ( $<0.1$ ) at frequencies around 1 THz. This indicates that 5CB and E7 in the nematic phase is potentially useful for device applications such as phase shifting in the THz frequency range.

In this Chapter, we demonstrate an electrically controlled liquid crystal THz phase shifter (Sec.3.3) and magnetically controlled liquid crystal THz phase shifters (Sec.3.4). The electric and magnetic fields are used to stabilize or change the orientation of LC molecules and hence the effective index of refraction for THz waves.

## 3.2. Theory

As we mentioned in Chapter 1, liquid crystals exhibit birefringent optical properties by virtue of the orientational order of anisotropic molecules. Like all crystals, the optical properties of liquid crystals depend on the direction of the propagation as well as the polarization state of the light-waves relative to the orientation of the liquid crystals.

Most of liquid crystal materials with rodlike molecules are optically uniaxial when an orientation order exists. In addition, most liquid crystal based device (ex. LCDs...) involve the use of nematic liquid crystals. A planar nematic slab is a good example of homogeneous uniaxial liquid crystal. Thus, the propagation of optic waves in uniaxially anisotropic media deserves special attention. The refractive indices associated with ordinary-ray and extraordinary-ray are given by

$$\text{o-ray: } n = n_o$$

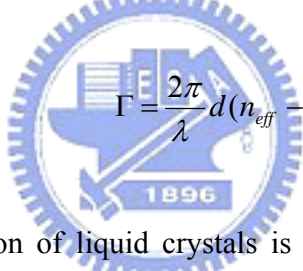
and

$$\text{e-ray: } \frac{1}{n_{eff}(\theta)^2} = \frac{\cos^2 \theta}{n_o^2} + \frac{\sin^2 \theta}{n_e^2} \quad (3.2.1)$$

where  $n_{eff}$  is the effective index and  $\theta$  is the angle between the direction of propagation and the optic axis. If the polarization of the electromagnetic wave is not right on the plane of optical axis and propagation direction, the relative optical path length difference, which is so-called retardation,  $\Lambda$ , is given by

$$\Lambda = d(n_{eff} - n_o), \quad (3.2.2)$$

and since  $\Gamma = k\Lambda$ , the phase difference, in radians, is

$$\Gamma = \frac{2\pi}{\lambda} d(n_{eff} - n_o). \quad (3.2.3)$$


The feature of the retardation of liquid crystals is usually used in application as a phase shifter/retarder, the filter, etc.

Nematic liquid crystals are well known as the birefringent materials, which can be oriented by surface molecular-scale structure, and extra field (electric field, magnetic field, etc). Once the direction of the liquid crystal molecules is changed, the effective indices related to the polarization of electromagnetic waves will also change according to Eq.(3.2.1). The change of the refractive indices will induce a phase shift or retardation (depend on that the polarization of electromagnetic wave.) The phase shift or retardation is given by

$$\delta = \frac{2\pi L f \Delta n_{eff}}{c} , \quad (3.2.4)$$

where  $L$  is the LC layer thickness,  $f$  is the frequency of THz wave,  $\Delta n_{eff}$  is the effective birefringence and  $c$  is the speed of light in vacuum. If the orientation of the LC molecules is not uniform, the effective birefringence, which is the function of the position in the liquid crystal layer, is shown as following

$$\delta = \int_0^L \frac{2\pi f}{c} \Delta n_{eff}(z) dz . \quad (3.2.5)$$

where  $L$  is the thickness of LC layer,  $\Delta n_{eff}$  is the change of effective birefringence,  $f$  is the frequency of the THz waves and  $c$  is the speed of light in vacuum.

### 3.3. Electrically-controlled liquid crystal terahertz phase shifter/retarder

#### 3.3.1. Design and sample preparation

Figure 3.3.1 schematically illustrates the configuration of a variable phase shifter using a nematic LC cell for phase shifting of THz signals propagating in free space. The cell was prepared by sandwiching the commercial available LC, 5CB (Merck), between two fused silica windows as substrates. The nominal thickness of the cell was 35  $\mu\text{m}$  by using Mylar of 35- $\mu\text{m}$ -thickness. The accurate thickness is measured by interference method as  $38.6 \pm 1.5 \mu\text{m}$ . Gold strips (one on each substrate), 3 mm in width and crossing at an angle of  $30^\circ$ , were deposited onto the inner surfaces of the substrates of the cell as electrodes. At the probing position, the strips were separated by about 3 mm. The cell was homogeneously aligned such that the director or optical-

axis of the LC was parallel to one of the gold strips. An ac voltage at 1 kHz was applied to the electrodes. Consider a linearly polarized THz beam passing through the cell with LC having positive dielectric anisotropy. Without any bias field or if the bias field (root mean square value) is smaller than a threshold value, the transmitted THz beam will remain linearly polarized if the polarization of the incident THz beam is parallel or perpendicular to the LC director. Once the bias field is larger than a threshold value, this bias field will reorient the direction of LC toward the bias field direction; this phenomenon is called a Fréedericksz transition [15]. As a result, the effective refractive index of the LC layer will change. The phase shift due to the electrically controlled birefringence is given by

$$\delta = \frac{2\pi L f \Delta n_{\text{eff}}}{c}, \quad (3.3.1.1)$$

where  $L$  is the LC layer thickness,  $f$  is the frequency of THz wave,  $\Delta n_{\text{eff}}$  is the average effective birefringence and  $c$  is the speed of light in vacuum.

### 3.3.2. Experiment and results

The device was characterized by THz time-domain spectroscopy. The experimental setup has been described (see Sec. 2.4.1). Briefly, the optical beam from a femtosecond mode-locked Ti:sapphire laser illuminated an inclined GaAs surface to generate the broad band THz signal, which was collimated and transmitted through the area between the two electrodes of the LC phase shifter. The transmitted THz signal was then detected by a probe beam from the same laser, using electro-optic sensing with a ZnTe crystal. The translation stage in our system is driven by a stepper motor with a 1  $\mu\text{m}$  step resolution (equivalent to a temporal resolution of 6.67 fs). The

measurements were done at room temperature (25 °C).

Figure 3.3.2.1(a) shows the incident and transmitted THz waveforms through the LC phase shifter without and with a bias field. The spectral width and center frequency of the incident THz pulse was 0.68 THz and 0.37 THz respectively. The total scan range for the time delay was 9.32 ps. In Fig. 3.3.2.1(a), we show the data from 0 to 9 ps. An expanded view of Fig. 3.2.2.1(a) in the time window of 5.28 to 5.34 ps can be seen in Fig. 3.3.2.1(b), in which the phase shift is evident from the time shift of the waveforms. The transmitted THz wave spectra were then obtained from the time-domain THz waveform by fast Fourier transform (FFT) algorithm. The values obtained for the phase shift of the THz beam by the LC phase shifter at various frequencies are plotted as a function of the bias field in Fig. 3.3.2.2. The threshold voltage required to rotate the LC occurs at  $\sim 35.4$  V (rms). The corresponding field was  $\sim 118.0$  V/cm. When the driving field is smaller than the threshold value, the nematic LC director will maintain their original uniform alignment. Therefore, no phase shift was observed. Once the bias field is larger than the threshold value, the effective refractive index of the LC will be changed until it is fully aligned with this field. The trend of phase shift versus bias field reflects this characteristic. That is, the phase shift rises steeply just above threshold and slowly approaches a steady state value. Under the same bias voltage, the terahertz wave experiences a larger phase shift at the higher frequencies in the 0.32 to 1.07 THz range.

### 3.3.3. Discussion and summary

According to Eq. (3.2.4), the phase shift is proportional to the product of the effective index change  $\Delta n_{eff}$  and frequency of the electromagnetic wave. Since  $\Delta n_{eff}$  is

$\sim 0.20$  in the range from 0.2 to 1.0 THz (see Chap. 2), we expect the observed phase shift to increase monotonically with frequency. The phase shift will reach a saturated value when the liquid crystal is completely aligned by the applied electric field. A maximum phase shift of  $4.07^\circ$  was obtained at 1.06 THz when the LC cell was driven at 589.3V/cm. The much larger phase shift is tentatively attributed to the Fabry-Perot effect due to multiple reflections of the THz wave transmitting through the cell. The thickness of the 5CB layer required to achieve a  $2\pi$  phase shift at 1 THz is  $\sim 1.4$  mm.

In summary, we have demonstrated a room temperature liquid-crystal-based THz phase shifter. The phase shift is achieved by electrical control of the effective refractive index of LC 5CB layer. A maximum phase shift of  $4.07^\circ$  was observed at 1.07 THz when the device was driven at 589.3 V/cm. In principle, the phase shift can be increased with a thicker LC cell and/or optimization of the electrode geometry.

### **3.4. Magnetically-controlled liquid crystal terahertz phase shifter/retarder**

#### **3.4.1. Design of the device**

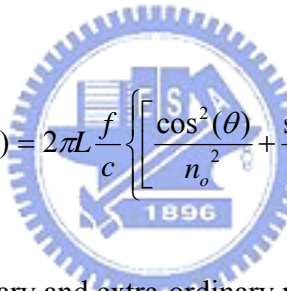
A schematic of the magnetically controlled THz phase shifter is shown in Fig. 3.4.1.1. The LC Phase shifter device consists of a homeotropic LC cell and a rotary magnet. The rotation axis is perpendicular to both of the polarization and the propagation directions of the THz wave. We define the magnetic inclination angle,  $\theta$ , as the angle between the magnetic field direction and the propagation direction. The effective refractive index of LC for THz waves changes with the molecular orientation,

which is controlled by the angle  $\theta$ . The phase shift,  $\delta(\theta)$ , due to magnetically controlled birefringence is given by

$$\delta(\theta) = \int_0^L \frac{2\pi f}{c} \Delta n_{eff}(\theta, z) dz, \quad (3.4.1.1)$$

where  $L$  is the thickness of LC layer,  $\Delta n_{eff}$  is the change of effective birefringence,  $f$  is the frequency of the THz waves and  $c$  is the speed of light in vacuum.

If the magnetic field is large enough, we can assume that the LC molecules are reoriented parallel to the magnetic field direction, the phase shift can then be re-written as



$$\delta(\theta) = 2\pi L \frac{f}{c} \left\{ \left[ \frac{\cos^2(\theta)}{n_o^2} + \frac{\sin^2(\theta)}{n_e^2} \right]^{\frac{1}{2}} - n_o \right\}, \quad (3.4.1.2)$$

where  $n_o$  and  $n_e$  are the ordinary and extra-ordinary refractive indices of the LC.

### 3.4.2. Sample preparation

Three cells have been used in this work. The structure of the first two cells with the nominal thicknesses of 1 and 2 mm is shown in Fig. 3.4.2.1(a). The actual thicknesses measured by a vernier caliper are 0.93, 1.32, respectively. The LC cells have 5CB (Merck) sandwiched between two fused silica plates with an area of 1 cm by 1 cm. The inner surfaces of the plates are coated with DMOAP (dimethyloctadecyl-(3-trimethoxysilyl)-propylammonium-chloride) such that the LC molecules are perpendicular to the substrates [16]. The other one, which is so called sandwich cell



(Fig. 3.4.2.1(b)), consists of three substrates with two layers of liquid crystal. The treatment of the four inner surfaces of the sandwich cell is the same as it of the mentioned cells. The filled liquid crystal is E7 (Daily Polymer Corp.)

For shifting the phase of the THz wave, we employ an Nd-Fe-B sintered magnet on a rotation stage. The magnetic field at the center of the LC cell is 0.51 Tesla, which is quite strong. The molecules of the liquid crystal will almost be parallel to the magnetic field within this strong field. The possible maximum magnetic inclination angle is  $55^\circ$ . Beyond that, the THz beam would be blocked by the magnet in the present setup.

### 3.4.3. Experiment and results

The device is characterized by THz-TDS. The experimental setup has been described in Sec. 2.4.1. Briefly, the optical beam from a femtosecond mode-locked Ti:sapphire laser illuminates a GaAs photoconductive antenna to generate the broad band THz signal, which is collimated and transmitted through the LC phase shifter. The transmitted THz signal is then detected by a probe beam from the same laser, using electro-optic sensing with a 4mm-thick (110) ZnTe crystal. The temporal resolution in our system is 6.67 fs. The measurements are done at room temperature ( $25^\circ\text{C}$ ).

#### 3.4.3.1. Single cell

The temporal THz profiles passing through the 1-mm-thick LC phase shifter at various magnetic inclination angles ( $\theta = 0^\circ, 30^\circ$  and  $50^\circ$ ) are illustrated in Fig.

3.4.3.1.1 with the notations of circle, open circle and triangle, respectively. The spectral width and center frequency of the incident THz pulse are 0.35 THz and 0.25 THz, respectively. The total scan range for the time delay was 9.58 ps, although only the data from 3 to 7 ps are shown. The transmitted THz waves for  $\theta > 0^\circ$  show obvious time delay to the THz wave for  $\theta = 0^\circ$ . The spectral amplitude and phase of the transmitted THz wave were deduced from the temporal waveforms by fast Fourier transform (FFT) algorithms. The phase shift due to the LC phase shifter at various frequencies are deduced and plotted as a function of the magnetic inclination angle in Fig. 3.4.3.1.2. The circles, open circles, triangles and open triangles are the measured data of the phase shift versus  $\theta$  at 1.025, 0.805, 0.512 and 0.293 THz, respectively. The curves are the theoretical predictions from Eq. 3.4.1.2, which agree with the data quite well. The maximum phase shift of  $108^\circ$  is achieved by using 1-mm-thickness cell. Figure 3.4.3.1.3 shows the measured phase shift versus the magnet angle  $\theta$  at 1.08 THz by using the 1.5-mm-thickness cell. The open circles are the measured data and the curve is the theoretical prediction. The maximum phase shift of  $141^\circ$  at  $\sim 1$  THz is achieved.

### 3.4.3.2. Sandwich cell

The temporal THz profiles passing through the LC phase shifter of the sandwich cell mentioned in Sec.3.4.2 at various magnetic inclination angles ( $\theta = 0^\circ$ ,  $30^\circ$  and  $50^\circ$ ) are shown in Fig. 3.4.3.2.1 with the notations of circles, open circles and triangles, respectively. The spectrum of the THz signal at  $\theta = 0^\circ$  is shown in the inset. The total scan range for the time delay was 12 ps, although only the data from 1 to 8.3

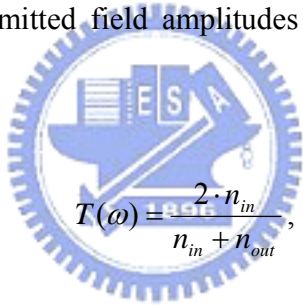
ps are shown. The transmitted THz waves show obviously longer time delay for larger angle,  $\theta$ . The phase shift by employing the sandwich cell versus the magnet angle,  $\theta$ , is shown in Fig. 3.4.3.2.2. The circles and the open circles are the measured phase shift at 0.49 and 1.025 THz and the curves are the theoretical predictions also from the Eq. 3.4.1.2. The LC filled in the sandwich cell is E7 and the maximum phase shift of  $368^\circ$  ( $>2\pi$ ) is achieved at the magnet angle of  $55^\circ$ .

### 3.4.4. Discussion

For the theoretical predictions of phase shift, we assume that all the molecules of LC are reoriented by such the strong magnetic field we used in this work. If the magnetic field is perpendicular to the alignment direction, a threshold field of 96.7 gauss is required to reorient LC molecules in our LC cell [15]. That threshold is much lower than the magnetic field employed in this work ( $\sim 0.51$  tesla). This means that Eq.4.3.1.2 is a reasonable assumption and can be used to predict the phase shifts. With Eq.4.3.1.2 and the previously measured ordinary and extraordinary indices of refraction of 5CB or E7 in the THz range (see Chap.2), we have calculated and plotted the theoretically predicted phase shifts in the figures as the solid curves. They show good agreements with the measured data. According to Eq.4.3.1.1, the phase shift is proportional to the product of the effective index change  $\Delta n_{eff}$  and frequency of the electromagnetic wave. The terahertz wave is thus expected to experience a larger phase shift at the higher frequencies in the measured THz range. This is also confirmed in Fig.3.4.3.1.2 and Fig.3.4.3.2.2. The maximum phase shifts of  $108^\circ$ ,  $141^\circ$  and  $368^\circ$  was obtained at  $\sim 1.0$  THz and  $\theta=55^\circ$  by using the 1-mm-thick, 1.5-mm-

thickness and the sandwich LC cells. A phase shift over  $2\pi$  is achieved by employing the sandwich cell.

In the above experiments, we also find that the THz field amplitudes increase with  $\theta$  for  $\theta < 43^\circ$ . This can be explained by the increasing transmittance at the quartz-LC interface according to the Fresnel equations [17]. The ordinary refractive indices ( $\sim 1.6$ ) of the LCs we used (5CB and E7) are smaller than the extraordinary indices ( $\sim 1.8$ ) at the frequency range of 0.2 to 1 THz. The refractive index of the fused quartz, which is used as the substrates is 1.951. With increasing  $\theta$ , the effective refractive index of LC will rise from  $n_o$  to  $n_e$  and become closer to the refractive index of quartz substrate (1.951). The transmitted field amplitudes will then increase according to Fresnel equations shown as

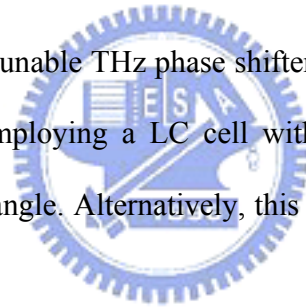


$$T(\omega) = \frac{2 \cdot n_{in}}{n_{in} + n_{out}}, \quad (3.4.4.1)$$

where the  $T(\omega)$  and  $\omega$  are the transmittance and the frequency of the electric field of the electromagnetic wave passing through the interface and the  $n_{in}$  and the  $n_{out}$  are the refractive indices of the materials, which are in incident-side and output-side, respectively. Here we ignore the dispersion of the materials and the imaginary part of the indices. Since both LCs we use and the fused silica have neglected dispersion and small imaginary indices. The THz field amplitudes decrease for  $\theta > 43^\circ$  due to partial blocking of the THz wave by the magnet.

### 3.4.5. Summary

In summary, we have demonstrated a room temperature liquid crystal THz phase shifter. The phase shift is achieved by magnetically controlling of the effective refractive index of LC layer. The magnetic field also helps to align the LC for cell as thick as 1.5 mm. Three cells, which are the 1-mm-thickness cell, 1.5-mm-thickness cell and the sandwich cell are employed in this work. The measured results are all in agreements with the theoretical predictions from Eq.4.3.1.2. In Eq. 4.3.1.2, we assume that all the molecules of LC are reorientated parallelly to the strong magnetic field discussed in Sec. 3.4.4. The maximum phase shifts of  $108^\circ$ ,  $141^\circ$  and  $368^\circ$  was obtained at  $\sim 1.0$  THz and  $\theta=55^\circ$  by using the 1-mm-thick, 1.5-mm-thickness and the sandwich LC cells. A phase shift over  $2\pi$  is achieved by employing the sandwich cell, which is a milestone of the tunable THz phase shifter. In principle, the phase shift can keep being increased by employing a LC cell with larger optical thickness and/or larger magnetic inclination angle. Alternatively, this can be also realized with a thinner LC cell with higher  $\Delta n$ .



## Bibliography

1. P. H. Siegel, *IEEE Trans. Microwave Theory Tech.* **50**, 910 (2002).
2. M. V. Exter, C. Fattinger, and D. Grischkowsky, *Opt. Lett.* **14**, 1128 (1989).
3. D. Grischkowsky, S. R. Keiding, M. V. Exter, and C. Fattinger, *J. Opt. Soc. Am. B* **7**, 2006 (1990).
4. B. B. Hu and M. C. Nuss, *Opt. Lett.* **20**, 1716 (1995).
5. R. A. Chevillie and D. Grischkowsky, *Appl. Phys. Lett.* **67**, 1960 (1995).
6. A. J. Fitzgerald, E. Berry, N. N. Zinovev, G. C. Walker, M. A. Smith, and J. M. Chamberlain, *Physics in Medicine and biology* **47**, R67 (2002).
7. C. Winnewisser, F. T. Lewen, M. Schall, M. Walther, and H. Helm, *IEEE Trans. Microwaves Theory Tech.* **48**, 744 (2000).
8. I. H. Libon, S. Baumgärtner, M. Hempel, N. E. Hecker, J. Feldmann, M. Koch, and P. Dawson, *Appl. Phys. Lett.* **76**, 2821 (2000).
9. R. Kersting, G. Strasser, and K. Unterrainer, *Electron. Lett.* **36**, 1156 (2000).
10. T. Kleine Ostmann, M. Koch, and P. Dawson, *Microwave Opt. Tech. Lett.* **35**, 343 (2002).
11. K. C. Lim, J. D. Margerum, and A. M. Lackner, *Appl. Phys. Lett.* **62**, 1065 (1993).
12. D. Dolfi, M. Labeyrie, P. Joffre, and J. P. Huignard, *Electronics Lett.* **29**, 926 (1993).
13. T.-R. Tsai, C.-Y. Chen, C.-L. Pan, R.-P. Pan, and X.-C. Zhang, *Appl. Opt.* **42**, 2372 (2003).

14. R.-P. Pan, T.-R. Tsai, C.-Y. Chen, C.-H. Wang, and C.-L. Pan, *Mol. Cryst. Liq. Cryst.* **409**, 137 (2004).
15. P. G. de Gennes and J. Prost, *The Physics of Liquid Crystals*. Oxford University, New York, 1993, Ch. 3.
16. F. J. Kahn, *Appl. Phys. Lett.*, **22**, 386 (1973).
17. Eugene Hecht, *Optics*, **3rd ed.** (Addison Wesley Longman, New York, 1998).



## Figure

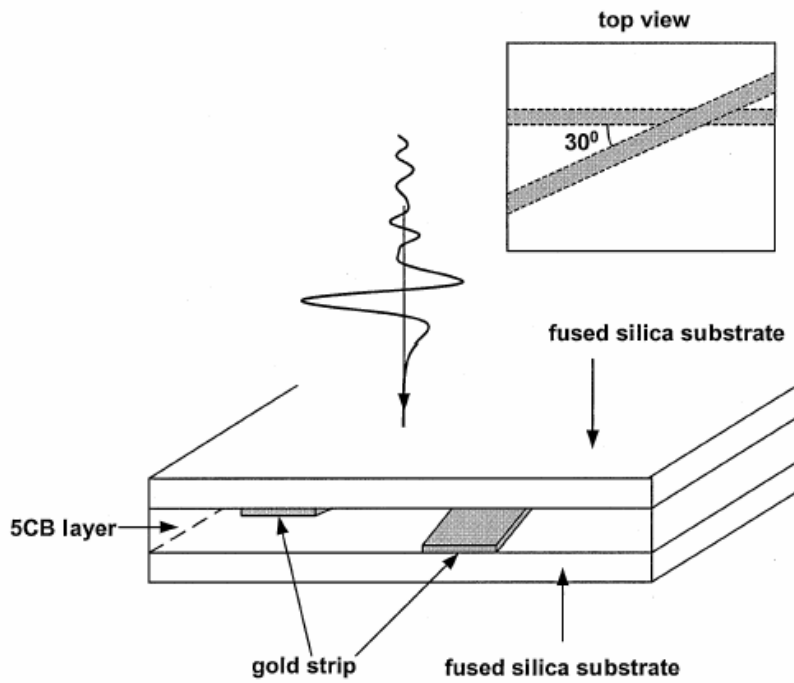
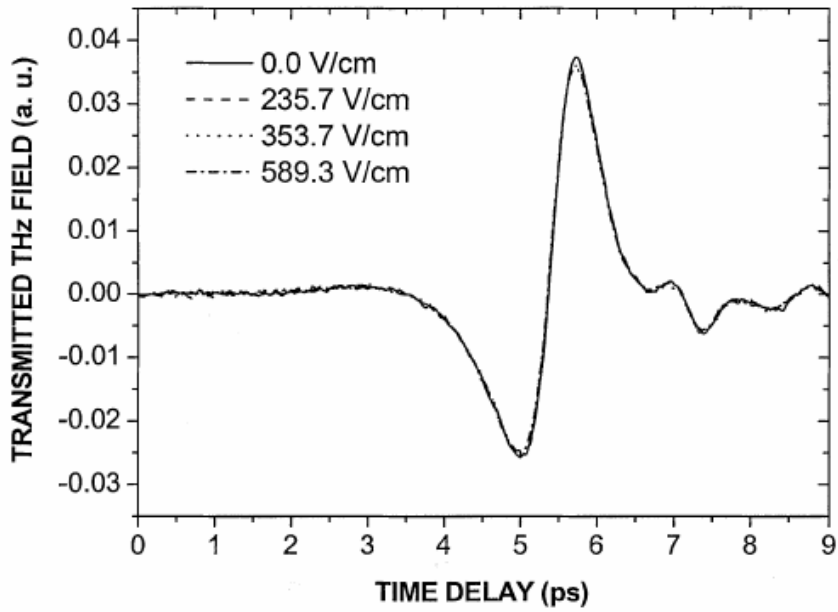
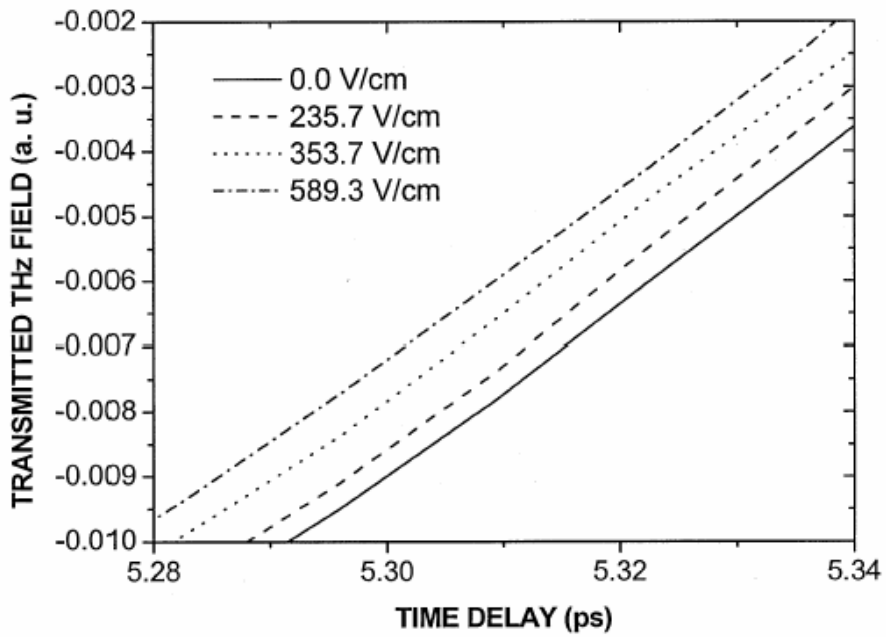


Figure 3.3.1 A schematic diagram of a THz phase shifter using a LC 5CB cell. The inset shows the top view of 5CB cell. The gray areas show the coated gold strips as the electrodes.





(a)



(b)

Figure 3.3.2.1 (a) The measured terahertz temporal waveforms transmitted through 5CB LC cell with various bias fields. (b) An expanded view of Fig. 2(a) in the time window of 5.28 to 5.34 ps.

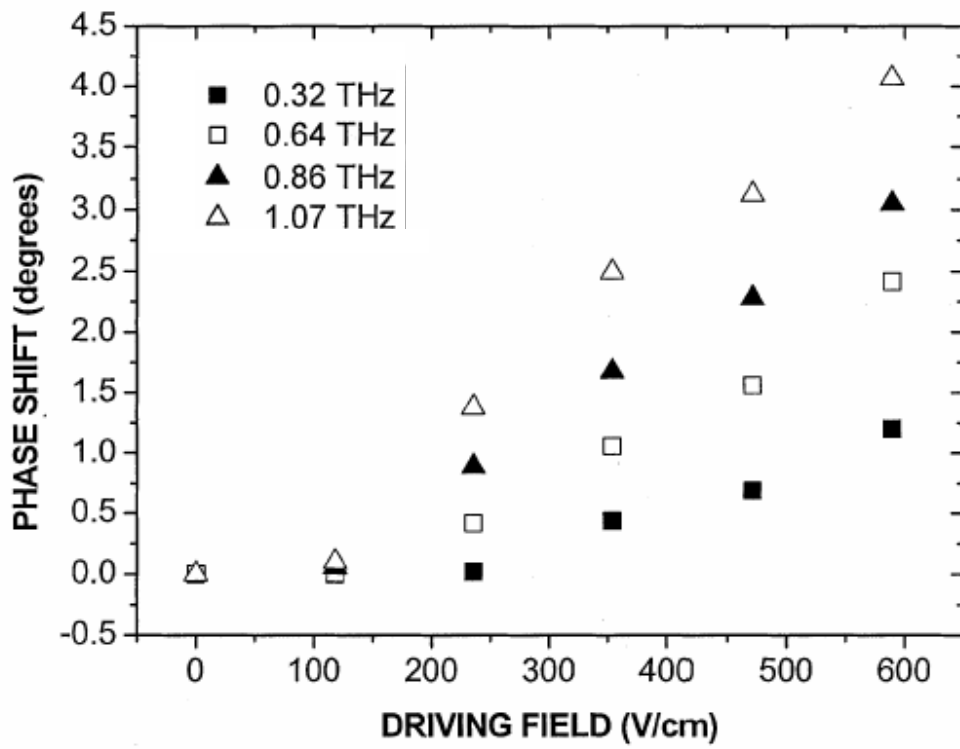


Figure 3.3.2.2 The phase shift of the terahertz wave against bias fields applied to 5CB cell.



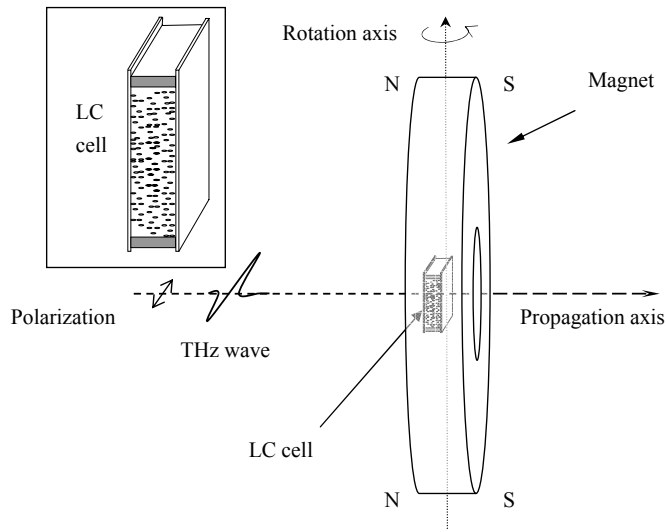


Figure 3.4.1.1 The schematic diagram of a THz phase shifter using a LC cell.

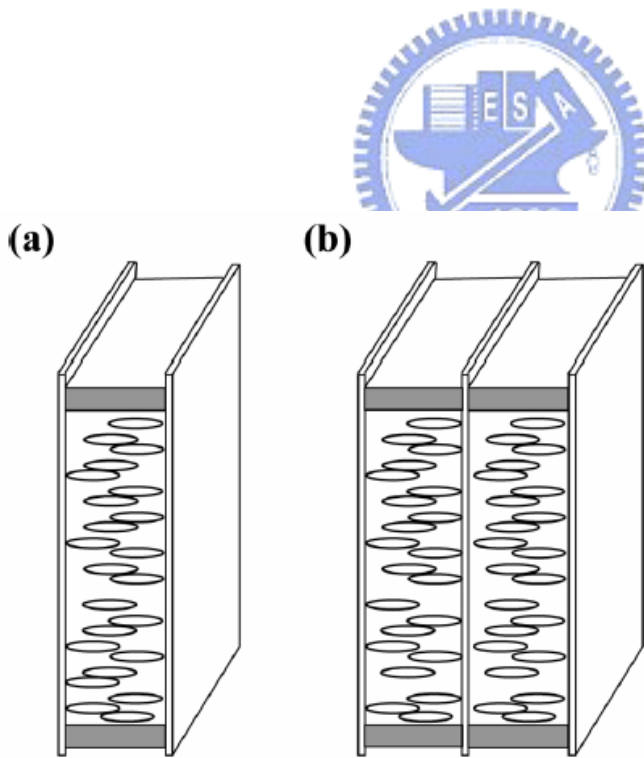


Figure 3.4.2.1 The structures of LC cells used in the THz phase shifter. The substrates are fused silica plates. The Teflon spacers are used for controlling the thickness. (a) The cell with one layer of LC, and (b) the cell with two layers of LC called sandwich cell.

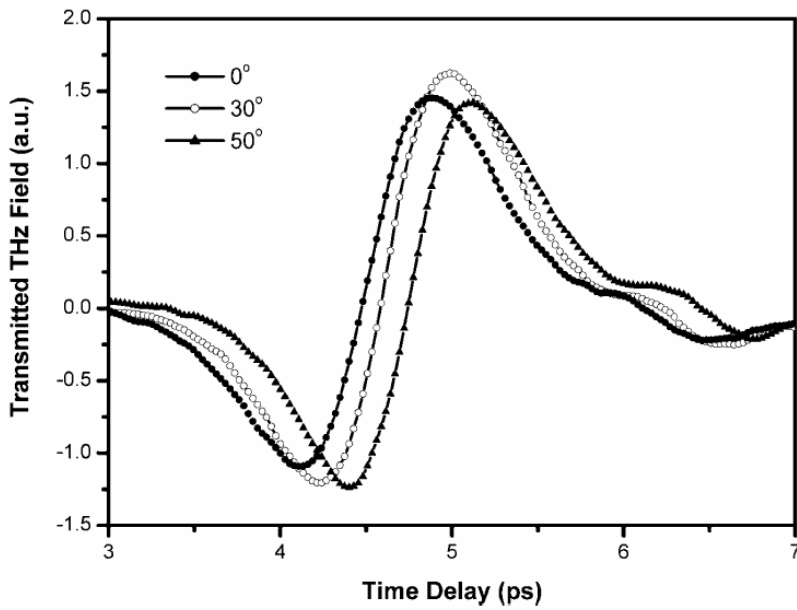


Figure 3.4.3.1.1 The measured THz waveforms transmitted through a 1-mm-thick 5CB LC cell at various magnetic inclination angles.

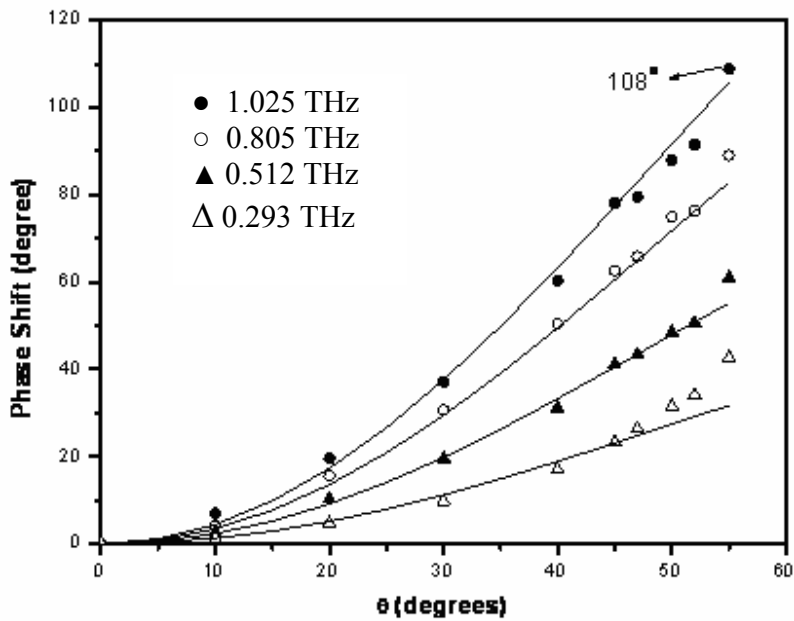


Figure 3.4.3.1.2 The phase shift of the THz waves passing through the 1-mm LC cell versus the magnetic inclination angle  $\theta$  at various frequencies. The solid curves are from the theoretical predictions. The symbols  $\bullet$ ,  $\circ$ ,  $\blacktriangle$  and  $\triangle$  correspond to experimental data at frequencies 1.025, 0.805, 0.512 and 0.293 THz, respectively.

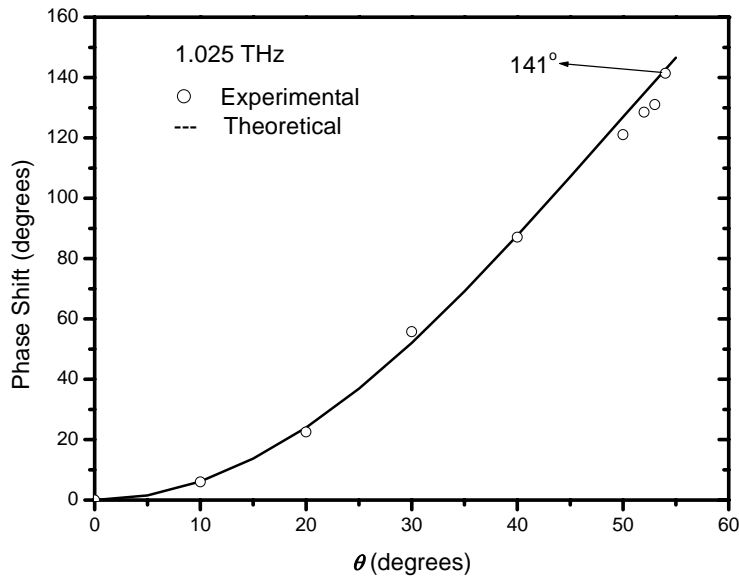


Figure 3.4.3.1.3 The phase shift of THz waves ( $f=1.025$  THz) passing through the 1.5-mm-thick LC cell versus the magnetic inclination angle.

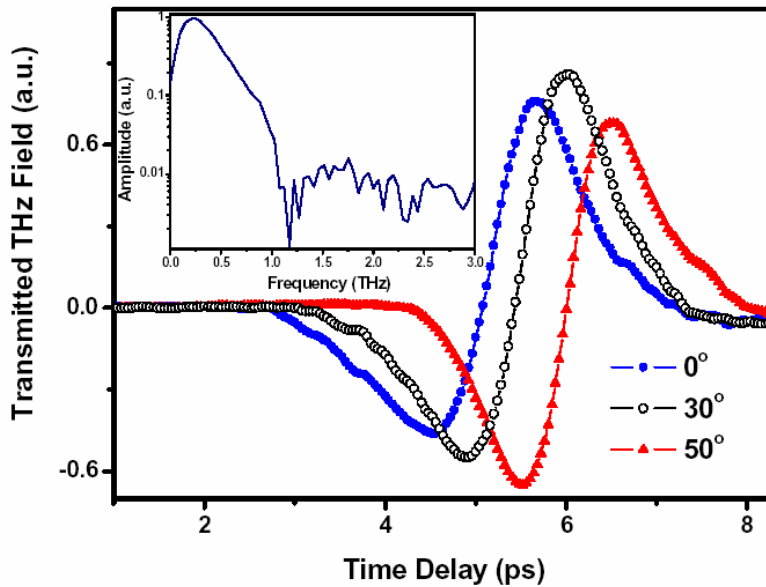


Figure 3.4.3.2.1 The measured THz waveforms transmitted through the LC phase shifter at various magnetic inclination angles. The inset shows the spectrum of the THz signal.

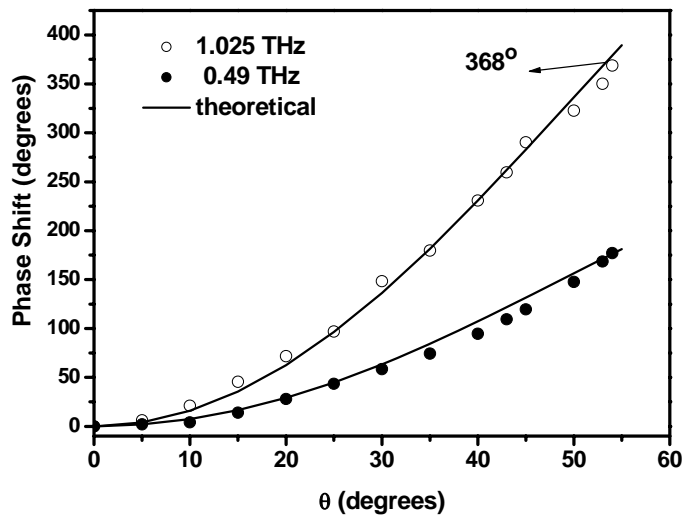


Figure 3.4.3.2.2 The phase shift of the THz waves versus the magnetic inclination angle. The solid curves are theoretical predictions. The open circles and circles are experimentally measured phase shift at 0.49 and 1.025 THz.

